water

MDPI

Article

Optimal Design of Water Distribution System Using Improved Life Cycle Energy Analysis: Development of Optimal Improvement Period and Unit Energy Formula

Yong min Ryu [1] and Eui Hoon Lee [2,*]

[1] Department of Civil Engineering, Chungbuk National University, Cheongju 28644, Republic of Korea; rmfl45@naver.com
[2] School of Civil Engineering, Chungbuk National University, Cheongju 28644, Republic of Korea
* Correspondence: hydrohydro@chungbuk.ac.kr; Tel.: +82-043-261-2407

Abstract: Water distribution systems (WDSs) are crucial for providing clean drinking water, requiring an efficient design to minimize costs and energy usage. This study introduces an enhanced life cycle energy analysis (LCEA) model for an optimal WDS design, incorporating novel criteria for pipe maintenance and a new resilience index based on nodal pressure. The improved LCEA model features a revised unit energy formula and sets standards for pipe rehabilitation and replacement based on regional regulations. Applied to South Korea's Goyang network, the model reduces energy expenditure by approximately 35% compared to the cost-based design. Unlike the cost-based design, the energy-based design achieves results that can relatively reduce energy when designing water distribution networks by considering recovered energy. This allows designers to propose designs that consume relatively less energy. Analysis using the new resilience index shows that the energy-based design outperforms the cost-based design in terms of pressure and service under most pipe failure scenarios. The implementation of the improved LCEA in real-world pipe networks, including Goyang, promises a practical life cycle-based optimal design.

Keywords: water distribution system; life cycle energy analysis; energy consumption; unit energy formula; new resilience index

check for updates

Citation: Ryu, Y.m.; Lee, E.H. Optimal Design of Water Distribution System Using Improved Life Cycle Energy Analysis: Development of Optimal Improvement Period and Unit Energy Formula. *Water* **2024**, *16*, 3300. https://doi.org/10.3390/w16223300

Academic Editors: Katarzyna Pietrucha-Urbanik and Janusz Rak

Received: 8 October 2024
Revised: 13 November 2024
Accepted: 15 November 2024
Published: 17 November 2024

1. Introduction

The supply of uncontaminated drinking water to consumers is essential for human life, and a water distribution system (WDS) is critical infrastructure to fulfill this necessity. The design of a WDS is complex because of its operational conditions and related uncertainties [1,2]. The design process involves determining several variables such as the pipe diameter, the pipe length between nodes, the pipe material, pumps, and tanks [3–6]. Various metaheuristic optimization algorithms have been used to derive optimal WDS designs [4,7–10]. Most of these studies have focused on minimizing the cost of designing a WDS [11–13]. Cost minimization studies aim to derive optimal designs based on the initial construction cost of a WDS but do not consider factors such as energy consumption during network construction. However, to construct a large-scale social infrastructure (such as a WDS), an optimal design should consider the entire life cycle, including maintenance and decommissioning.

The life cycle includes the entire process from fabrication to the disposal of any item or facility [14,15]. The major stages to be considered during the WDS life cycle are fabrication, maintenance, and disposal. While the fabrication and disposal stages analyze the static condition of the entire facility, the maintenance stage considers the aging and destruction of pipes over time. Shamir and Howard (1979) confirmed that pipe destruction occurs exponentially and proposed a failure rate formula [16]. Sharp and Walski (1988) derived a simple formula for pipe aging over time using the Hazen–Williams and Darcy–Weisbach equations [17]. Mononobe (1960) proposed a destruction estimation formula based on existing WDS data [18]. Shamir and Howard (1979) proposed a method for planning pipe replacement cycles in a WDS based on the degree of destruction, and Male et al. (1990) suggested a cost-effective method for renewal and replacement cycles in a WDS [16,19]. Studies on the maintenance stages of WDSs and those considering environmental and economic factors based on WDS life cycle analysis have also been conducted [16,19]. Subsequently, the life cycle energy analysis (LCEA) model has been applied to WDSs [12,20]. Representative WDS optimal design studies using LCEA include the study by Filion et al. (2004) and the study by Lee et al. (2015) [14,21].

In this study, a new LCEA was proposed that improved the shortcomings of Filion et al. (2004) and Lee et al. (2015), which are representative LCEA studies [14,21]. In the case of the newly proposed LCEA, to apply it without modifying the basic data of the pipe network to be applied, the C value of the existing pipe network was used, and the C value of the newly buried pipe was equally applied during rehabilitation and replacement. To enhance applicability, a method was employed to calculate rehabilitation and replacement times, considering regional characteristics based on local regulations and pipe C values. In addition, to improve the accuracy of the unit energy calculation formula in the process of improving applicability, a new optimal unit energy calculation formula was proposed by analyzing various types of trend lines and R^2 according to the trend lines. Additionally, a novel resilience index was formulated and applied to assess the performance of the proposed water distribution system design using the new LCEA model. The new resilience index, developed based on Todini's (2000) and Cimellaro et al.'s (2016) resilience indices primarily used in water distribution systems (WDSs), was introduced [22,23]. The previously proposed resilience index integrated factors like the affected population in a system failure, the tank capacity in the WDS, and water quality through calculations [22,23]. The new resilience index focuses on the need to restore water pressure at each node to meet WDS standards for a return to the original state after a failure. The new resilience index presented in this study employs an approach that assesses the overall system performance by considering hydraulic pressure at each node during failure events. Through the utilization of this new resilience index, a comparative analysis was conducted between the cost-based optimal design plan and the energy-based optimal design plan.

2. Methodology

2.1. Overview

This study consisted of four main parts. First, metaheuristic optimization algorithms (MOAs) were selected for the optimal WDS design. Second, optimal improvements and renewal timing based on the aging of the WDS were established. Third, the LCEA model was analyzed using a new unit energy calculation method. Finally, a new resilience index was developed and applied based on the pressure at each node in the water pipe network. The optimal design search method using the improved LCEA method used in this study is shown in Figure 1.

According to Figure 1, the first step is to establish the optimal improvement and regeneration period according to the aging of the WDS. The WDS consists of multiple pipes. For each pipe, the optimal diameter is selected from among various types of diameters. In order to establish the optimal rehabilitation, repair, and replacement period, it is necessary to calculate the degree of aging according to the diameter for each pipe, and the criteria are presented based on this. The second step is to select MOAs. MOAs have been developed in the past, but each has its own advantages and disadvantages. For example, there are MOAs with a small number of parameters and high usability and MOAs with a large number of parameters and internal operators but low usability but good performance. Among the MOAs developed previously, MOAs that showed good performance in the WDS optimal design were selected and applied to the WDS optimal design through parameter sensitivity analysis. The third step is to develop a new unit energy calculation method. In order to improve the accuracy of the existing unit energy calculation method, various unit energy calculation formulas were established, and the optimal unit energy calculation formula was proposed through accuracy analysis. Finally, a new resilience index was developed. Based on the optimal design produced through the proposed method, a new resilience index was developed, applied, and evaluated to analyze the resilience of the design when a disaster occurs.

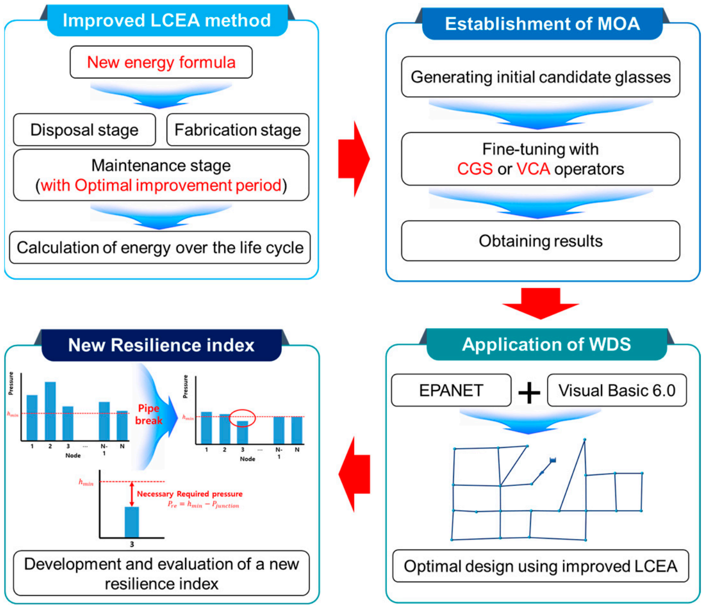

Figure 1. Optimal design search method using improved LCEA model.

2.2. Metaheuristic Optimization Algorithm for Optimal Water Distribution System Design

The optimal design of a WDS consists of deriving an optimal design plan according to the designer's purpose while satisfying the user's requirements such as appropriate water quality and demand. Traditionally, this approach has relied on trial and error based on user experience, with additional mathematical techniques applied [24]. Since 1981, research has been conducted using linear and nonlinear functions to design WDSs to minimize the cost of branched pipe networks [25–27]. However, in the case of linear and nonlinear functions, an optimal design could not be derived due to nonlinear elements in the simulation process and dependence on the initial solution group [6,28,29]. To overcome the limitations of these mathematical techniques, metaheuristic algorithms have been used for WDS optimization [11,30–32]. Among various metaheuristic algorithms, the modified hybrid vision correction algorithm (MHVCA) has demonstrated superior performance in minimizing costs for WDS optimization [10].

In this study, among various metaheuristic optimization algorithms, the modified hybrid vision correction algorithm (MHVCA) proposed by Ryu and Lee (2023) was used [10]. The MHVCA is a metaheuristic optimization algorithm that consists of six parameters that must be set by the user. According to Ryu and Lee (2023), the MHVCA showed good results in the optimal design of six WDSs (Goyang network, Hanoi network, Pescara Network, Zhejiang network, Modena network, and Balerma network) and showed better results than metaheuristic optimization algorithms such as Harmony search and the Genetic algorithm, which have fewer parameters than the MHVCA [10]. In this study, the effectiveness of the MHVCA in WDS optimization was used to explore the optimal design of WDSs to minimize energy consumption. Table 1 provides a description of each important internal operator and parameter used in the MHVCA.

According to Table 1, the CGS, CGSR, and DR are probability parameters for operator selection, while the CF, AF, MTF, and MHR are parameters utilized to fine-tune the solution during iterative calculations. The optimal solution search process of the MHVCA is as follows in Figure 2.

Table 1. Important internal operators and parameters in the MHVCA [10].

Operators (Full Name)	Description	
CGS (Centralized Global Search)	An operator that proceeds with a search after setting a new search range using the optimal value of the current iteration and the median value of the search range	-
MTF (Modulation Transfer Function)	A method for adjusting the decision variable based on the distance between the best value among the existing optimal solutions and the new solution using an operator that mimics lens brightness adjustment in the process of manufacturing glasses	
Parameters (Full name)	**Description**	**Value of range (General value)**
MHR (Modified Hybrid Rate)	A parameter used in the process of searching for a new solution, a probability parameter that determines whether fine-tuning (search method using CF, AF, and MTF) is executed	0~0.36 (Self-adaptive)
CGSR (Centralized Global Search Rate)	Probability parameter that determines whether CGS is executed	0~1 (Self-adaptive)
CF (Compression Factor)	A method of reducing the range of region search as the number of iterations increases with an operator that mimics the compression process in the process of manufacturing glasses	0~100 (30)
AF (Astigmatic Correction)	A method of setting and searching the range of region search based on the angle of the astigmatism axis set by the user with an operator that mimics the astigmatism correction process in the process of manufacturing glasses	0~180 (45)
DR (Division Rate)	A probability parameter that determines the direction to be searched within the search range during the process of searching for a new solution	0~1 (0.1)

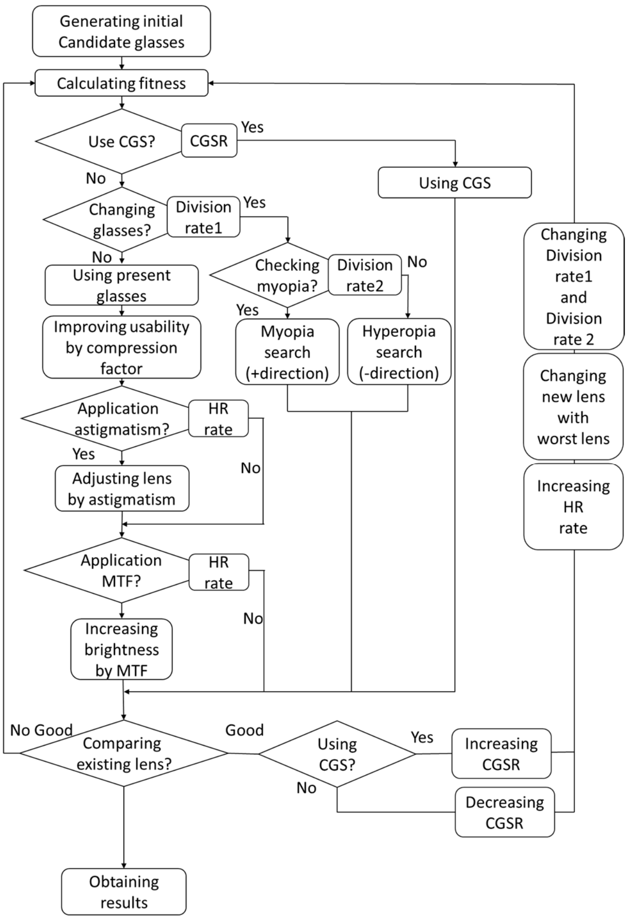

Figure 2. Flowchart of MHVCA.

According to Figure 2, the MHVCA does not search for the number of solution combinations equal to the number of parent generations like the Genetic algorithm in one optimal solution search, but it instead searches for one solution combination (glasses in MHVCA terminology).

2.3. Establishment of Optimal Improvement Period

In the pursuit of cost minimization, the optimal WDS design requires alternatives with minimal initial installation costs. However, to analyze the WDS life cycle, it is essential to consider the energy required for maintenance over time after pipeline installation. Therefore, to simulate the maintenance of a WDS, it is crucial to proactively model the aging of pipes over time. Lee et al. (2015) quantified the Hazen–Williams coefficient (C) based on the equation proposed by Mononobe (1960) and the coefficient proposed by Baek (2002), which is expressed as follows [14,18,33]:

$$C_y = C_0\left(1 - \frac{(0.0961659\mathrm{D} + 1.15507)\sqrt{y}}{D}\right)^{0.723076D^{-0.0660117}} \tag{1}$$

where C_y denotes the C value over time, C_0 denotes the initial C value, D denotes the diameter of the pipe (mm), and y denotes the year after burial or replacement.

A previous study used Equation (1) to propose the rehabilitation and replacement period for pipes, which were suggested based on the value of the Hazen–Williams coefficient (C). When C was ≤ 90, the pipe was rehabilitated; after two rehabilitations, if C was $\leq$80, the pipe was replaced. It was assumed that C recovered to 90–110 after rehabilitation and to 130 after replacement because of the installation of new pipes. However, in this study, the rehabilitation and replacement periods of pipes were not set uniformly based on a fixed value of C. Instead, a method was proposed to consider the Hazen–Williams coefficient (C) of the WDS under consideration. The service life of the water supply and sewage facilities was specified based on the regulations of the Office of Waterworks in South Korea. The WDS used in this study was the Goyang network. In order to estimate the head loss of a pipe, the Darcy–Weisbach or Hazen–Williams formula is used. In the case of the Goyang network, which is the water pipe network applied in this study, the head loss was estimated using the Hazen–Williams formula as a result of analyzing the initially proposed literature and the literature in which the optimal design was conducted [4,10,13,34,35]. Therefore, in this study, the Hazen–Williams formula was also used to conduct the optimal design. The material of pipe that constitutes the Goyang network is assumed to be made of steel according to the existing literature, and the useful service life of the pipe is set to 30 years [10,13,34,35]. Therefore, based on the diameter of the pipes, rehabilitation and replacement criteria were established using the C value after 30 years (useful life for the service of steel pipes). Figure 3 shows the variation in C values by diameter over time.

As shown in Figure 3, after 30 years, the C values for each pipe range from approximately 60 to 68. To establish criteria for rehabilitation and replacement, the average C value for pipes after 30 years was set to about 65 in this study. Furthermore, based on the existing replacement criteria, replacement was performed after two rehabilitation sessions. To determine the recovered C values following rehabilitation and replacement, an approach similar to that proposed in previous studies was adopted. Similarly to previous research, it was assumed that after rehabilitation, the C value of pipes recovered to approximately 85% of their initial C values (130 out of 110).

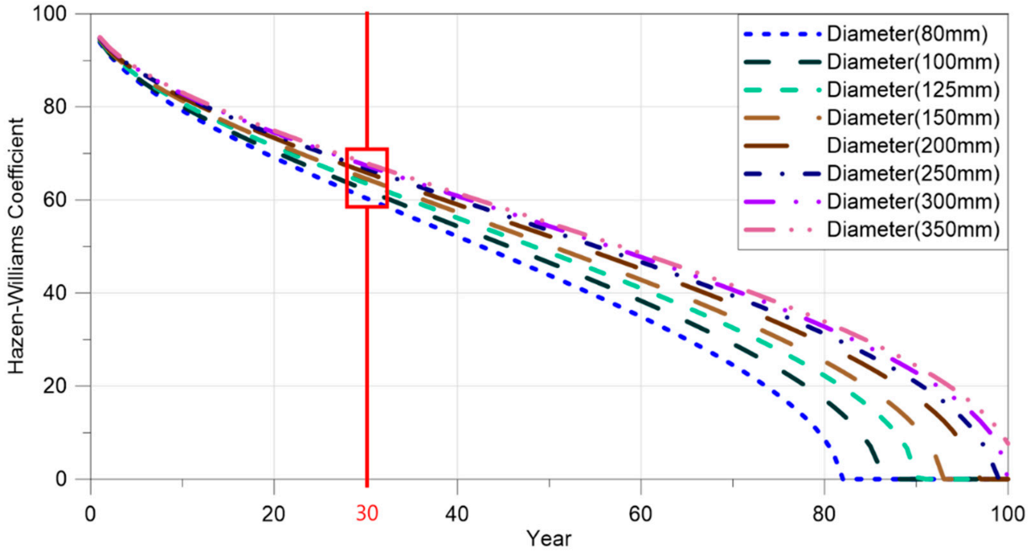

Figure 3. Convergence curve of C by diameter over time (red box is distribution of C according to diameter after 30 years.).

2.4. The LCEA Model Using a New Unit Energy Equation

The proposed LCEA model can be divided into three main phases—Phase 1 determines the rehabilitation period of each pipe using information on the WDS to be optimized (pipe diameters) and regulations specific to the region; Phase 2 calculates the unit energy for each pipe using the WDS information to be optimized (nodes, pipes, pressures, etc.); Phase 3 is further divided into three stages (fabrication, maintenance, and disposal). During the fabrication stage, the fabrication energy of all pipes in the WDS can be calculated using the unit energy. The maintenance stage involves estimating the maintenance energy over the intended life cycle by considering pipe destruction simulations and the rehabilitation period determined in Phase 1. Finally, the disposal stage involves calculating the disposal energy for all pipes in the WDS using unit energy. The improved LCEA model was simulated using Visual Basic 6.0 and EPANET 2.0 (US EPA, 2000) [36]. In this study, Demand-Driven Analysis (DDA) and Pressure-Driven Analysis (PDA) were used in the process of applying EPANET to optimally design the WDS. DDA was used to simulate normal situations for optimal design, and PDA was used to simulate abnormal situations for resilience index analysis [10,37–40]. This study calculated the resilience index based on the optimal design and optimal design plan. In the process of conducting the optimal design, the optimal design plan was derived using the DDA method. PDA was used to calculate the disaster resilience index of each optimal design plan. The demand at each node of the WDS to be applied was set as a fixed value, and the temporal distribution pattern of demand was not applied. The optimal WDS design using the LCEA model can be used to calculate the annual energy consumption. Using this, the year with the lowest energy consumption can be set to be the optimal life cycle. The objective function of the optimal WDS design using the LCEA model can be expressed as follows:

$$E_{all} = \left[E_{fab} + (E_{main} - E_{rec}) + E_{dis} + Penalty\right]/LC \quad (2)$$

where E_{all} denotes the total annual energy (GJ/year), E_{fab} denotes the fabrication energy (GJ/year), E_{main} denotes the maintenance energy (GJ/year), E_{rec} denotes the recycle energy (GJ/year), E_{dis} denotes the disposal energy, *Penalty* denotes the penalty function, and *LC* denotes the optimal life cycle (year). The penalty function can be used to exclude design proposals that do not satisfy the minimum required hydraulic pressure of each node during the process of optimal WDS design. On the one hand, if the minimum required water pressure is satisfied, the penalty is zero; on the other hand, if the minimum required water pressure is not satisfied, a penalty is assigned, as follows:

$$\begin{gathered} Penalty = \sum_{jc=1}^{tot} 10^{20} \times \left(h_{minP} - h_{jc}\right) + 10^{7}, \left(if\ h_{jc} < h_{minP}\right) \\ Penalty = 0, \left(if\ h_{jc} > h_{minP}\right) \end{gathered} \tag{3}$$

where tot denotes the total number of nodes in the WDS, h_{minP} denotes the minimum water pressure of the nodes in the WDS, and h_{jc} denotes the water pressure of jc.

2.4.1. New Unit Energy Equation

For an optimal WDS design using the LCEA model, the energy generated at each stage (fabrication, maintenance, and disposal) must be analyzed, which is based on the length of the pipe. To calculate the unit energy based on diameter, it is essential to ensure accuracy by building on the previously suggested values. In this study, various formulas for unit energy calculations were expressed using trend equations, and an optimal formula for the unit energy calculation was proposed. The trend equation was established using previously studied data, and the diameter data of the Goyang pipe network were utilized to analyze the possibility of additional use. Table 2 presents unit energy equations using existing unit energy equations and various proposed equations and is a table showing the R^2 value for each equation.

Table 2. Previously proposed unit energy formula and various other formulas.

	Previous Function [14]	$\mathbf{R^2}$
Fabrication	$e_{fab} = \left(4.206 \times D^{1.9959}\right) \times \text{Conv}$	0.9962
Disposal	$e_{dis} = \left(0.2974 \times D^{2.0248}\right) \times \text{Conv}$	0.9952
	Linear function	$\mathbf{R^2}$
Fabrication	$e_{fab} = (27.053 \times D - 35.659) \times \text{Conv}$	0.9788
Disposal	$e_{dis} = (1.9904 \times D - 2.6401) \times \text{Conv}$	0.9789
	Log function	$\mathbf{R^2}$
Fabrication	$e_{fab} = (78.805 \times \ln(D) - 31.34) \times \text{Conv}$	0.9298
Disposal	$e_{dis} = (5.8014 \times \ln(D) - 2.326) \times \text{Conv}$	0.9308
	Exponential function	$\mathbf{R^2}$
Fabrication	$e_{fab} = \left(4.2905 \times D^{1.9677}\right) \times \text{Conv}$	0.9992
Disposal	$e_{dis} = \left(0.3035 \times D^{1.9927}\right) \times \text{Conv}$	0.9989
	2nd-order polynomial function	$\mathbf{R^2}$
Fabrication	$e_{fab} = \left(4.3669 \times D^2 - 2.0038 \times D + 3.1002\right) \times \text{Conv}$	0.9962
Disposal	$e_{dis} = \left(0.3116 \times D^2 - 0.0831 \times D + 0.1258\right) \times \text{Conv}$	0.9952
	3rd-order polynomial function	$\mathbf{R^2}$
Fabrication	$e_{fab} = \left(2.1678 \times D^3 - 19.535 \times D^2 + 65.506 \times D - 58.322\right) \times \text{Conv}$	0.9963
Disposal	$e_{dis} = \left(0.1769 \times D^3 - 1.476 \times D^2 + 5.427 \times D - 4.8875\right) \times \text{Conv}$	0.9979
	4th-order polynomial function	$\mathbf{R^2}$
Fabrication	$e_{fab} = \left(1.2748 \times D^4 - 15.24 \times D^3 + 62.27 \times D^2 - 107.33 \times D + 64.24\right) \times \text{Conv}$	1.0000
Disposal	$e_{dis} = \left(0.1116 \times D^4 - 1.3474 \times D^3 + 5.9498 \times D^2 - 9.7072 \times D + 5.8445\right) \times \text{Conv}$	1.0000

In this table, D denotes the pipe diameter (m), and $Conv$ denotes a unit conversion factor that converts m units to GJ/m. As shown in Table 2, the R^2 values for the previously proposed unit energy formulas are 0.9962 and 0.9952. For the previously proposed function, regression analysis was performed based on five data points, and the function was expressed as an exponential function [14,21]. In this study, various analyses were performed based on the five given data points in the same way as the method used in the existing literature. However, when various functions (linear, log, exponential, and polynomial) were used to calculate the unit energy, the 4th-order polynomial function had the highest R^2 value of 1.0000 for the unit fabrication and disposal energy. However, because of the uniqueness of the polynomial function, when calculating the unit energy using pipes from locations other than those proposed by Filion et al., the energy decreased as the pipe diameter increased [21]. In the case of individual pipes forming a constant pipe, as the diameter increases, the energy required to manufacture the pipe increases. However, in the case of the 4th-order polynomial presented in Table 2, when data other than the given data are input, the energy required to manufacture the pipe decreases. Consequently, considering the specific nature of the polynomial function, it was excluded from the unit energy formula. An exponential function that realized the highest R^2 value was chosen for the new unit energy formula. The proposed unit fabrication and disposal energy formula can be expressed as follows:

$$e_{N\_fab} = \left(4.2905 \times D^{1.9677}\right) \times \text{Conv} \tag{4}$$

$$e_{N\_dis} = \left(0.3035 \times D^{1.9927}\right) \times \text{Conv} \tag{5}$$

where e_{N_fab} denotes the new fabrication unit of energy, e_{N_dis} denotes the new disposal unit of energy, D denotes the pipe diameter (m), and Conv denotes a unit conversion factor that converts m units to GJ/m.

2.4.2. Energy Calculation for Design of Water Distribution System

As mentioned in Section 2.4.1, for the optimal design of WDSs employing LCEA, it is imperative to calculate the energy generated during the fabrication, maintenance, and disposal stages. In this study, the energy for each stage, as suggested by Lee, was computed using the newly proposed unit energy calculation formula based on the diameter [41]. The energy calculation formula for each stage, which integrates the newly proposed unit energy calculation formula, is presented in Table 3.

Table 3. Energy calculation formula and description for each stage [41].

Stage	Formula	Description
Fabrication	$E_{fab} = \sum_{i=1}^{Tot} L_i \times 4.2905 \times D^{1.9677}$	This stage includes various processes such as raw material extraction, material processing and production, and pipe fabrication. The energy consumed in these processes can be defined as the fabrication energy.
Maintenance	$E_{main} = \left(E_{reh} + E_{rep} + E_{rpi}\right) - E_{rec}$ $E_{reh} = \sum_{i=1}^{Tot} L_i\left(N_{reh} \times 0.65 \times 4.2905 \times D^{1.9677}\right)$ $E_{rep} = \sum_{i=1}^{Tot} L_i\left(N_{rep} \times 4.2905 \times D^{1.9677}\right)$ $E_{rpi} = \sum_{i=1}^{Tot} L_i \times N(t) \times \left(2 \times L_b \times 4.2905 \times D^{1.9677}\right)$ $E_{rec} = \frac{1}{pump_e} \sum_{i=1}^{Tot} \left(E_{p,i}^{p} - E_{p,i}^{a}\right)$	The maintenance process of a WDS comprises the rehabilitation, repair, and replacement of pipes, owing to aging or pipe failure. Maintenance energy defines all the energy consumed during the maintenance stage. Lee et al. (2015) defined recycling energy as the benefit obtained from the improved flow rate resulting from the rehabilitation of pipes during the maintenance process [41].
Disposal	$E_{dis} = \sum_{i=1}^{Tot} L_i \times 0.3035 \times D^{1.9927} \times \left(1 + N_{reh}\right)$	The disposal stage involves the disposal of pipes that constitute the WDS. Disposal energy is the energy consumed purely for the disposal of pipes, which includes the energy required for the disposal of pipes during replacement as well as that consumed during the disposal of pipes in the maintenance stage.

In this table, E_{fab} denotes the fabrication energy consumption (GJ), Tot denotes the total number of pipes, L_i denotes the length of the ith pipe (m), D denotes the diameter of the pipe, E_{main} denotes the maintenance energy consumption (GJ), E_{reh} denotes the rehabilitation energy (GJ), E_{rep} denotes the replacement energy (GJ), E_{rpi} denotes the repair energy (GJ), E_{rec} denotes the recycled energy (GJ), N_{reh} denotes the number of pipe rehabilitations, N_{rep} denotes the number of pipe replacements, *N(t)* denotes the pipe failure probability function, L_b denotes the typical breakage length, $pump_e$ denotes the efficiency of the pump, $E^p_{p,i}$ denotes the pump energy required when the pipe is rough before rehabilitation, and $E^a_{p,i}$ denotes the pump energy required when the pipe is smooth after rehabilitation.

2.5. Development of New Resilience Index Using Insufficient Pressure

A new resilience index was proposed to evaluate and compare the performance of the proposed design using the improved LCEA. Using the new resilience index, we evaluated the performance of the WDS design through scenarios such as system failure caused by natural disasters. The proposed new resilience index is an index that can indicate the performance of the system based on the pressure per node within the WDS, based on the resilience proposed by Cimellaro et al. (2016) [23]. The proposed new resilience index is as follows.

$$R = R_1 \times R_2 \times R_3 \times R_P \tag{6}$$

$$R_1 = \sum_{T_L=0}^{LC} \frac{1-\frac{\sum_i n^i_{p,e}}{n_{Tot}}}{T_L} \text{for i} = 1,2,\cdots,\text{n}, R_2 = \sum_{T_L=0}^{LC} \frac{F_{(t)}}{T_L}, F_{(t)} = \begin{cases} \frac{h(t)}{h_{Reserve}} h \leq h_{reserve} \\ 1\ h > h_{reserve} \end{cases},$$
$$R_3 = \sum_{T_L=0}^{LC} \frac{\frac{Q(t)}{Q^*}}{T_L}, R_P = \sum_{T_L=0}^{LC} \frac{1-\frac{\sum_j^{Nan}\left(h_{min}-h_{jun}\right)}{\sum_j^{Ntn} h_{min}}}{T_L} \tag{7}$$

where T_L is the control time (life cycle), $n^i_{p,e}$ is the number of users receiving insufficient pressure, n_{Tot} is the number of users in the WDS, n is the number of nodes affected by the outage, *h(t)* is the tank water level at time *t*, $h_{Reserve}$ is the reserve capacity of the tank, *Q(t)* is the water quality at time *t*, Q^* is the water quality factor, Ntn is the total number of nodes, h_{min} is the minimum required water pressure, Nan is the number of abnormal nodes, and h_{jun} is the pressure of node *j*. Additionally, R_1 is the number of households affected by a water outage in the event of a system failure due to a natural disaster, etc., which is proportional to the system serviceability index proposed by Todini (2000) [22]. In the case of R_1, if it is assumed that no failure occurs in the WDS when a natural disaster occurs, it can be represented as 1, and if a failure occurs at all nodes in the WDS, it can be represented as 0 [22]. R_2 is a proposed index based on the water level of the tank in the network, R_3 is a factor for water quality, and R_4 is a newly proposed resilience index calculated through all nodes and abnormal nodes within the WDS. In the case of R_2, if there is a tank in the WDS and the reserve capacity in the tank is higher than the tank water level at time t, it can be represented as 1, and in the opposite case, the value of the index is calculated according to the ratio of the tank water level at time t to the reserve capacity in the tank. R_3 is the ratio of the water quality concentration to the bad concentration at time t due to the occurrence of a natural disaster. Therefore, if it does not meet the water quality standard, it will have a value between 0 and 1 depending on the result. R_4 is a coefficient that quantifies the pump energy required to restore a disaster situation according to the reduced pressure at each node in the WDS due to the occurrence of a natural disaster. R_4 has a value less than 1 when the pressure at each node decreases due to a natural disaster and has a value of 0 when the pressure at all nodes is 0%. R_1~R_4 are coefficients for indexing the resilience of the system to a disaster situation when a natural disaster occurs and a failure occurs in the WDS, and they always have a value less than 1 for an abnormal situation where a problem occurs within the WDS. If no failure occurs in the WDS, the resilience index has a maximum value of 1, and if the WDS does not function as intended, it has a minimum value of 0.

3. Results

3.1. Study Area

The Goyang network located in South Korea was selected as the target area for the energy optimization design using the improved LCEA model. The layout of the Goyang network is shown in Figure 4.

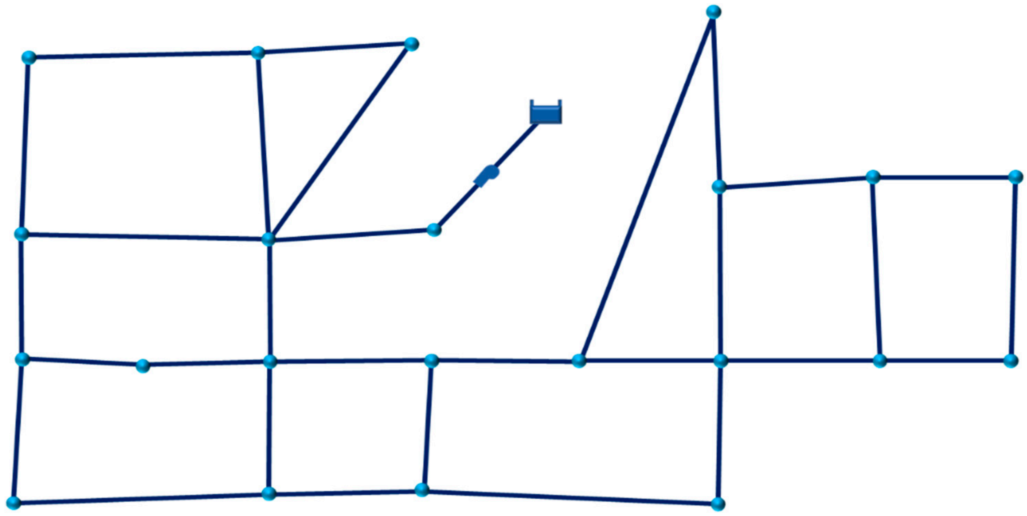

Figure 4. Layout of Goyang network.

The Goyang network comprises 1 reservoir, 25 nodes, and 30 pipes. The Hazen–Williams coefficient for calculating the head loss of the Goyang network was set to 100. The minimum water pressure required for each node in the Goyang network was 15 m. Table 4 lists the pipe diameter and cost per pipe diameter used for the optimal design of the Goyang network.

Table 4. Cost per unit length based on diameter.

Diameter (mm)	Cost (USD/m)	Diameter (mm)	Cost (USD/m)	Diameter (mm)	Cost (USD/m)	Diameter (mm)	Cost (USD/m)
80	37.890	125	40.563	200	47.624	300	62.109
100	38.933	150	42.554	250	54.125	350	71.524

3.2. Optimal WDS Design Using Improved LCEA Model

In this study, the proposed LCEA model was used to analyze the difference between energy- and cost-based optimal designs. There are a total of six parameters (CG, CGSR, DR_1, DR_2, CF, and AF) that need to be set for the MHVCA. Among the parameters of the MHVCA, candidate glasses (CG) are the storage space within the algorithm. The parameters of the MHVCA were selected through sensitivity analysis, and Table 5 shows the parameters of the MHVCA set to apply the MHVCA to the Goyang network.

Table 5. Values for each parameter of MHVCA.

Parameter	Value
CG	190
CGSR	0
DR_1	0.1
DR_2	0.7
CF	30
AG	45

The optimal design was performed using the MHVCA with parameters set according to Table 5. The optimal design was performed according to cost- and energy-based optimal designs, and the results showing the best value after 30 uses of each optimal design were analyzed. Table 6 shows the results of the optimal design of the Goyang network used 30 times using a cost-based design and energy-based design. Table 6 shows the results of the optimal design of the Goyang network used 30 times using a cost-based design and energy-based design.

Table 6. Comparison of cost and energy for each optimal design.

Analysis by Cost	Cost-Based Design	Energy-Based Design
Mean cost (USD)	177,064.779	177,492.181
Best cost (USD)	177,010.359	177,010.359
Worst cost (USD)	177,020.938	177,141.106
Standard deviation	21.172	130.392
Analysis by energy	**Cost-based design**	**Energy-based design**
Mean energy (GJ)	805.549	578.210
Best energy (GJ)	757.747	478.317
Worst energy (GJ)	788.369	535.783
Standard deviation	9.480	21.034

According to Table 6, in terms of cost, the best cost of the both cost-based design and energy-based design was the same at 177,010.359, which was the optimal value. However, the mean cost of the cost-based design was 177,020.938, and that of the energy-based design was 177,141.106, which was higher than that in the energy-based design. In terms of energy, the mean energy of the energy-based design was about 252.586 lower than that of the cost-based design, and the best energy was about 279.429 lower. The standard deviation was higher in the energy-based design than in the cost-based design, but based on the comparison of the best energy, worst energy, and mean energy, it can be seen that the energy-based design shows better results in terms of energy. Figure 5 shows the convergence curves according to the cost-based and energy-based optimal designs in terms of cost, and the convergence curves are expressed as the average of the results of 30 uses.

According to Figure 5, in the case of the cost-based design, it can be seen that it converges quickly and converges after about 2500 iterations. However, it can be seen that the energy-based design converges after about 6000 iterations. Figure 5 shows that the purpose of the optimal design is to minimize cost. Therefore, it can be seen that the cost-based design converges to a lower value than the energy-based design. Figure 6 shows the convergence curves according to the cost-based and energy-based optimal designs in terms of energy, and the convergence curves are expressed as the average of the results of 30 uses.

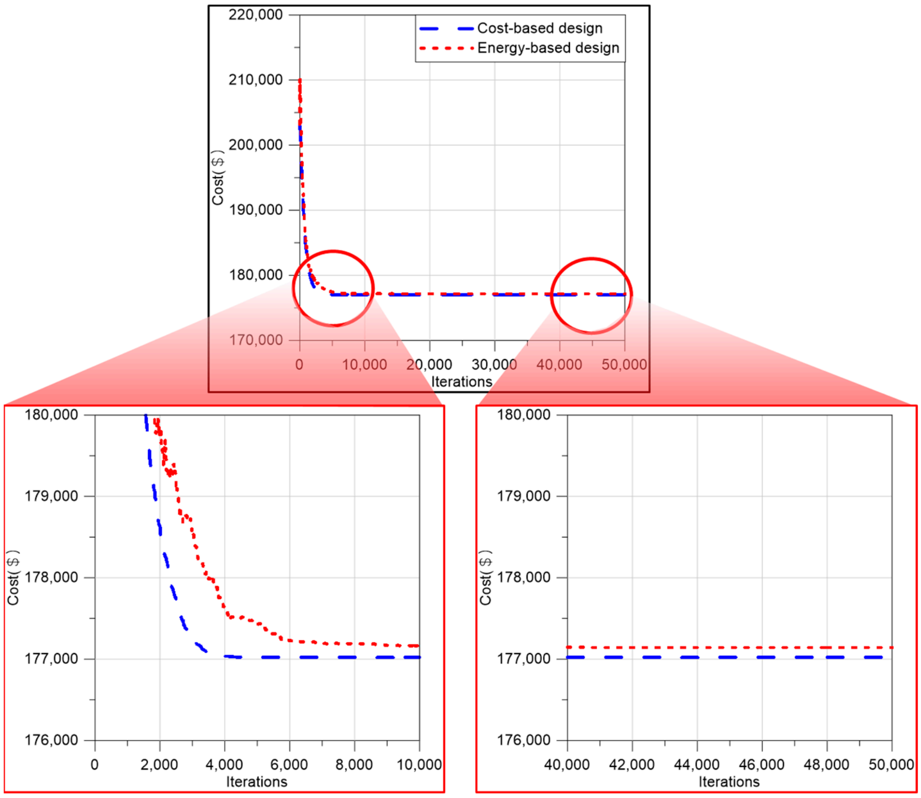

Figure 5. Convergence curves for optimal design in terms of cost.

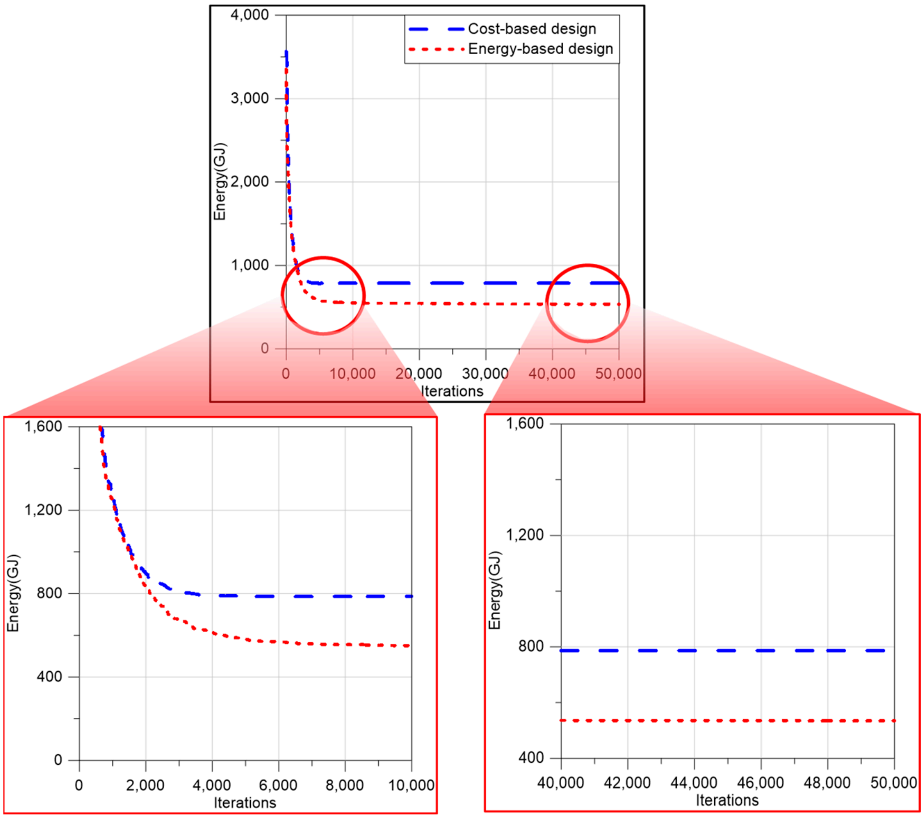

Figure 6. Convergence curves for optimal design in terms of energy.

According to Figure 6, in the case of the cost-based design, it can be seen that it converges quickly and then converges after about 4000 iterations. However, in the case of the energy-based design, it can be seen that it converges after about 8000 iterations, but it can be seen that it converges to a lower value than the cost-based design. Figure 5 shows that the purpose of the optimal design is to minimize energy. Therefore, it can be seen that the energy-based design converges to a lower value than the cost-based design. Table 7 shows the pipe diameters by the location of the design plan that showed the best results among the optimal design results of the cost-based design and energy-based design that were used to minimize energy.

Table 7. Pipe diameters by location of design plan.

Location	Pipe Diameter (mm) Cost-Based Optimal Design	Pipe Diameter (mm) Energy-Based Optimal Design	Location	Pipe Diameter (mm) Cost-Based Optimal Design	Pipe Diameter (mm) Energy-Based Optimal Design
1	47.624	47.624	16	37.89	37.89
2	40.563	42.554	17	37.89	37.89
3	40.563	38.933	18	37.89	37.89
4	38.933	38.933	19	37.89	37.89
5	37.89	37.89	20	37.89	37.89
6	37.89	37.89	21	37.89	37.89
7	37.89	37.89	22	37.89	37.89
8	37.89	37.89	23	37.89	37.89
9	37.89	37.89	24	37.89	37.89
10	37.89	37.89	25	37.89	37.89
11	37.89	37.89	26	37.89	37.89
12	37.89	37.89	27	37.89	37.89
13	37.89	37.89	28	37.89	37.89
14	37.89	37.89	29	37.89	37.89
15	37.89	37.89	30	37.89	37.89

According to Table 7, we can see that the design plans for the cost-based design and energy-design are different in locations 2 and 3. In the case of the cost-based design, the same pipe was used in locations 2 and 3 to minimize cost, and in the case of the energy-based design, different pipes were used in locations 2 and 3 to minimize energy.

Table 8 presents the results of the cost- and energy-based optimal designs using the MHVCA based on the WDS in the study area.

Table 8. Cost- and energy-based optimal design results using MHVCA.

	Cost-Based Optimal Design	Energy-Based Optimal Design
Total energy expenditure * (GJ)	805.549	494.769
Total energy expenditure per year (GJ/year)	33.565	20.615
Life cycle (year)	24	24
E_{fab} (GJ)	173.730	174.560
E_{reh} (GJ)	418.806	426.196
E_{rpi} (GJ)	24.623	0.000
E_{rep} (GJ)	173.730	174.560
E_{dis} (GJ)	23.195	23.310
E_{rec} (GJ)	8.535	303.858
Cost per year (USD/year)	7375.432	7377.704
Cost (USD)	177,010.359	177,064.903

Note(s): * Total energy expenditure is sum of all consumed energies ($E_{all} = E_{fab} + (E_{reh} + E_{rep} + E_{rpi} - E_{rec}) + E_{dis}$).

According to Table 8, the energy-based optimal design achieves approximately 39% more energy savings compared to the cost-based design, with a total energy expenditure difference of about 310.779 GJ. On an annual basis, the energy-based design leads to savings of approximately 24.949 GJ compared to the cost-based design throughout the life cycle. While the cost-based design exhibits lower fabrication, rehabilitation, repair, and disposal energies, the energy-based design excels in repair energy efficiency. Focused on minimizing energy consumption, the energy-based design results in lower repair energies during the maintenance stage. Moreover, the energy-based design outperforms in recycled energy during maintenance, with around 303.858 GJ compared to the cost-based design's approximately 8.535 GJ. The E_{fab} of the energy-based optimal design is 0.48% higher than that of the cost-based optimal design, and in the case of E_{dis}, it is about 0.49% higher. Unlike the cost-based optimal design, the energy-based optimal design is a design method for reducing CO_2 emissions. The energy-based optimal design considers the amount of carbon generated during maintenance stages such as rehabilitation and repair during the life cycle. Therefore, the energy-based optimal design derives an optimal design by selecting a pipe with a relatively large diameter. This is because pipes with a large diameter decrease less in aging over time than pipes with a small diameter. However, the energy-based optimal design has a lower E_{rep} than the cost-based optimal design. Based on the results of E_{rep}, it can be seen that the energy-based optimal design can use WDSs without replacement because it uses pipes with a relatively large diameter. In addition, the E_{rec} of the energy-based optimal design is about 35 times higher than that of the cost-based optimal design. It can be seen that the optimal design of the energy-based optimal design recovers more energy than the optimal design of the cost-based optimal design, and in terms of energy, the energy-based optimal design is better than the cost-based optimal design. E_{rpi} is lower in the energy-based optimal design than in the cost-based optimal design. The probability of pipe failure is calculated according to the diameter. The energy-based optimal design uses larger pipes than the cost-based optimal design, and this shows that the energy-based optimal design has a lower probability of pipe failure in areas where failure mainly occurs. E_{rep} is the same as E_{fab} for each design method. Erep is the energy generated when replacing a pipe. Therefore, if all individual pipes in the WDS reach the pipe replacement point, all pipes are replaced. Since the life cycle is longer than the pipe replacement point, all pipes are replaced, producing the same result as E_{fab}. Figure 7 shows the results of the cost- and energy-based optimal designs based on the consumed energy.

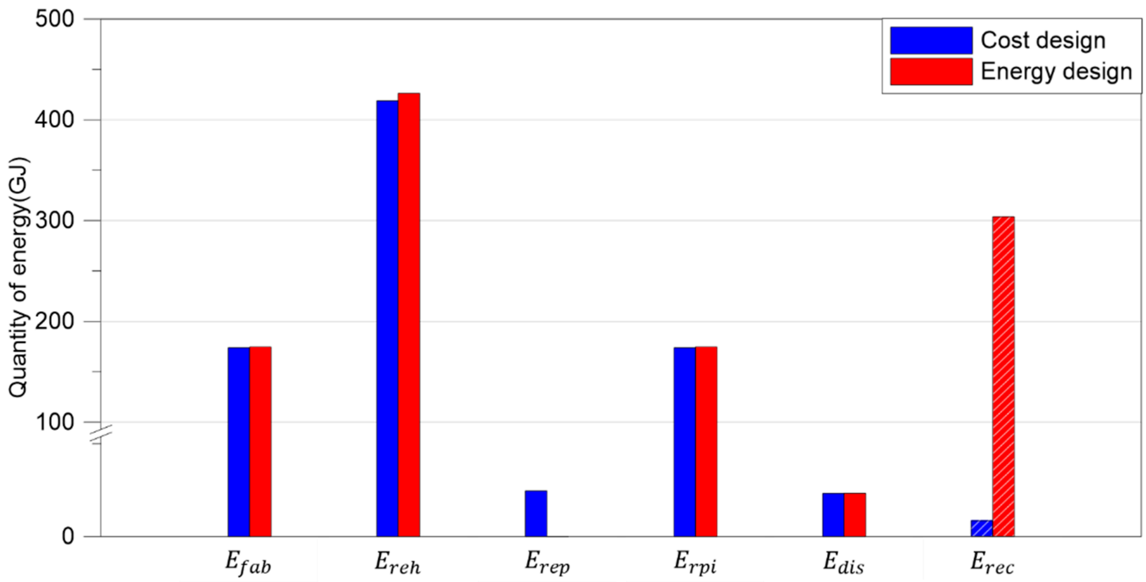

Figure 7. Energy consumption by optimal design methods.

It is evident that the energy-based design results in higher values for E_{fab}, E_{reh}, E_{rpi}, and E_{dis} compared to the cost-based design. However, the energy-based design exhibits a considerably lower E_{rep} value than that of the cost-based design. The E_{rec} plot (represented by the diagonal lines) in Figure 6 indicates that higher recycled energy values lead to improvements in energy efficiency gains. The energy-based design exhibits considerably higher E_{rec} values than those of the cost-based design. Moreover, Figure 7 shows that the energy-based design performs optimization based on various energy consumption values and, overall, is more effective in achieving energy savings compared to the cost-based design.

In this study, the proposed LCEA model was used to analyze the results of energy- and cost-based optimal designs for the Goyang network. The analysis revealed that the energy-based optimal design showed lower total energy expenditure and total energy expenditure per year than the cost-based optimal design. To conduct additional analysis, the benefits of reducing energy consumption were converted into costs. To convert energy savings into costs, all fuels used during the Goyang network's life cycle were assumed to be petroleum-based. A method of converting energy into kWh and subsequently into costs was employed, as suggested by the Korea Energy Economics Institute (KEEI), and the settlement unit prices for each fuel type provided by the Korean Statistical Information Service (KOSIS) were used [42,43]. According to the KEEI, 1 GJ is equivalent to 277.8236 kWh, and according to the KOSIS, the cost per 1 kWh is KRW 299.78. Additionally, recent exchange rates were used to convert KRW to USD. By applying this conversion method, the energy consumption results shown in Table 5 were analyzed based on the energy- and cost-based optimal designs. When implementing the energy-based optimal design for the Goyang network, approximately USD 20,526.22 was saved compared to the cost-based optimal design, with an annual saving of USD 855.26. However, the direct application of the results, obtained by converting energy into costs using the current exchange rate, was not entirely accurate, owing to potential fluctuations in the exchange rate.

Based on the energy-based and cost-based optimal designs, the new resilience and pipe failure scenarios proposed were established and applied to compare the performance of each design. In the failure simulation of the WDS, various failure scenarios, such as single-pipe failure and multiple-pipe failure, can be established [24]. According to Beker and Kansal, it was mentioned that when natural disasters such as earthquakes and landslides occur, multiple pipe failures rarely occur [44]. Jung et al. (2014) simulated single-pipe failure conditions after optimization, and Pagano et al. (2019) evaluated the impact of single-pipe failure in the water pipe network [45,46]. Therefore, in this study, resilience according to failure was calculated using failure scenarios for all pipes of the energy-based and cost-based optimal designs for the Goyang pipe network. Based on each design plan, PDA was performed using EPANET 2.2. To simulate PDA using EPANET 2.2, the minimum pressure was set to 0, required pressure was set to 15, which is the minimum required water pressure of the Goyang pipe network, and the pressure component was set to 0.5 [47,48].

Since the Goyang network used in this study is a network with no reservoir within the network, R_2 was assumed to be 1. In the case of water quality, R_3 was assumed to be 1, assuming that all factors subject to water quality testing are maintained above the standards set by the law [23]. Additionally, in the case of the population affected by a water outage, it was assumed that the same population lives at all nodes. The pipe failure scenario was constructed as a single-pipe failure scenario for the pipes existing in the WDS from the first pipe to the final pipe. Table 9 is a table presenting the resilience calculated according to the scenario based on each optimal design.

According to Table 9, the energy-based optimal design yielded high or equal resilience results in all but three scenarios. Upon calculating the average of resilience indices, it was determined to be approximately 0.8377 for the cost-based optimal design and around 0.8512 for the energy-based optimal design. The energy-based design showed a maximum increase of approximately 9.2176% in the resilience index compared to the cost-based design and an average increase of approximately 1.95%. Both the overall and average results indicate that the energy-based optimal design outperforms the cost-based optimal design in terms of disaster recovery. This suggests that the energy-based optimal design possesses a superior ability to restore the system to its original state in the event of a disaster compared to the cost-based optimal design.

Table 9. Comparison of resilience between cost-based and energy-based optimal designs by scenario.

Pipe Failure Scenario	Cost-Based Optimal Design (A)	Energy-Based Optimal Design (B)	Difference (%)	Pipe Failure Scenario	Cost-Based Optimal Design (A)	Energy-Based Optimal Design (B)	Difference (%)
1	0.0000	0.0000	0	16	1.0000	1.0000	0.0000
2	0.1490	0.1548	3.7628	17	1.0000	1.0000	0.0000
3	0.4975	0.5001	0.5263	18	1.0000	1.0000	0.0000
4	0.4807	0.4831	0.4893	19	0.9544	1.0000	4.5599
5	0.8055	0.8526	5.5220	20	0.9079	0.9543	4.8716
6	0.7996	0.8050	0.6776	21	1.0000	1.0000	0.0000
7	0.8941	0.8953	0.1262	22	0.8062	0.8083	0.2669
8	0.9041	0.9048	0.0852	23	0.8054	0.8116	0.7576
9	0.9078	1.0000	9.2176	24	0.9023	0.9063	0.4498
10	0.9543	1.0000	4.5744	25	0.9541	1.0000	4.5888
11	1.0000	1.0000	0.0000	26	0.8096	0.8118	0.2779
12	1.0000	1.0000	0.0000	27	0.8479	0.8496	0.1972
13	0.9077	0.9545	4.9062	28	1.0000	1.0000	0.0000
14	1.0000	1.0000	0.0000	29	0.8936	0.8947	0.1170
15	1.0000	1.0000	0.0000	30	0.9494	0.9500	0.0639

4. Discussion

In this study, sensitivity analysis was performed on each parameter of the MHVCA used. A total of six parameters were subjected to sensitivity analysis. Sensitivity analysis was conducted by setting initial values for CG, CGSR, DR_1, DR_2, CF, and AF based on previous studies and then applying various values to analyze the results and select values. Sensitivity analysis was performed 10 times in total with the goal of cost minimization, and the maximum cost, minimum cost, mean cost, and standard deviation were compared and analyzed to set the values. Tables 10–15 show the results of sensitivity analysis and selected values for each parameter.

Table 10. CG sensitivity analysis results and parameter value selection.

	100	**110**	**120**	**130**	**140**	**150**
Mean Cost (USD)	177,071.823	177,015.813	177,021.255	177,064.903	177,015.636	177,031.778
Best Cost (USD)	177,010.359	177,010.359	177,010.359	177,010.359	177,010.359	177,010.359
Worst Cost (USD)	177,294.363	177,064.903	177,064.903	177,026.697	177,063.124	177,064.903
Standard Deviation	78.212	16.363	21.793	24.957	15.830	26.253
Selection						
	160	**170**	**180**	**190**	**200**	**-**
Mean Cost (USD)	177,026.521	177,026.685	177,031.600	177,015.427	177,026.158	-
Best Cost (USD)	177,010.359	177,010.359	177,010.359	177,010.359	177,010.359	-
Worst Cost (USD)	177,064.903	177,064.779	177,064.903	177,061.038	177,064.903	-
Standard Deviation	24.692	24.938	26.033	15.204	24.149	-
Selection				O		-

Table 11. CGSR sensitivity analysis results and parameter value selection.

	0	**0.1**	**0.2**	**0.3**	**0.4**	**0.5**
Mean Cost (USD)	177,015.427	177,029.236	177,784.975	179,523.054	183,325.455	184,490.049
Best Cost (USD)	177,010.359	177,014.772	177,583.053	178,884.215	181,980.392	183,364.440
Worst Cost (USD)	177,061.038	177,064.903	178,028.545	180,156.294	184,345.112	185,891.822
Standard Deviation	15.204	22.111	134.937	396.245	707.003	877.799
Selection	O					
	0.6	**0.7**	**0.8**	**0.9**	**1.0**	**-**
Mean Cost (USD)	184,521.035	192,010.403	191,279.585	194,634.407	198,455.637	-
Best Cost (USD)	182,186.073	188,093.943	182,095.278	190,812.490	195,333.524	-
Worst Cost (USD)	187,807.926	194,201.503	194,767.095	197,291.409	201,015.790	-
Standard Deviation	1532.913	1933.878	3502.999	1826.033	1872.217	-
Selection						-

Table 12. DR_1 sensitivity analysis results and parameter value selection.

	0	**0.1**	**0.2**	**0.3**	**0.4**	**0.5**
Mean Cost (USD)	177,119.522	177,015.427	177,015.813	177,015.813	177,015.801	177,015.813
Best Cost (USD)	177,061.038	177,010.359	177,010.359	177,010.359	177,010.359	177,010.359
Worst Cost (USD)	177,216.720	177,061.038	177,064.903	177,064.903	177,064.779	177,064.903
Standard Deviation	57.427	15.204	16.363	16.363	16.326	16.363
Selection		O				
	0.6	**0.7**	**0.8**	**0.9**	**1.0**	**-**
Mean Cost (USD)	177,015.813	177,015.813	177,015.813	177,033.023	177,015.801	-
Best Cost (USD)	177,010.359	177,010.359	177,010.359	177,010.359	177,010.359	-
Worst Cost (USD)	177,064.903	177,064.903	177,064.903	177,236.998	177,064.779	-
Standard Deviation	16.363	16.363	16.363	67.992	16.326	-
Selection						-

Table 13. DR_2 sensitivity analysis results and parameter value selection.

	0	**0.1**	**0.2**	**0.3**	**0.4**	**0.5**
Mean Cost (USD)	177,199.296	177,039.121	177,043.797	177,042.471	177,036.864	177,031.753
Best Cost (USD)	177,014.772	177,010.359	177,010.359	177,010.359	177,010.359	177,010.359
Worst Cost (USD)	177,828.255	177,085.639	177,072.511	177,064.779	177,064.779	177,064.779
Standard Deviation	222.011	29.482	27.392	26.242	26.523	26.222
Selection						
	0.6	**0.7**	**0.8**	**0.9**	**1.0**	**-**
Mean Cost (USD)	177,020.881	177,015.427	177,026.697	177,015.801	177,021.255	-
Best Cost (USD)	177,010.359	177,010.359	177,010.359	177,010.359	177,010.359	-
Worst Cost (USD)	177,064.903	177,061.038	177,064.903	177,064.779	177,064.903	-
Standard Deviation	21.062	15.204	24.957	16.326	21.793	-
Selection		O				-

According to Tables 10–15, since the CGSR, DR_1, and DR_2 of the parameters of the MHVCA are probability parameters, sensitivity analysis was conducted in units of 0.1, and CG, CF, and AF were analyzed by creating about 11 to 13 cases depending on the range of parameters generally applied. When proceeding with the optimal design of the Goyang pipeline using the MHVCA, it can be seen that the best result was shown when CG = 190, CGSR = 0, DR_1 = 0.1, DR_2 = 0.7, CF = 30, and AF = 45. The MHVCA set with the values of the corresponding parameters was mostly the same as the MHVCA applying other parameters in terms of the minimum cost, but the maximum cost was lower, and it could be confirmed that this led to the lowest standard deviation.

Table 14. CF sensitivity analysis results and parameter value selection.

	0	10	20	30	40	50
Mean Cost (USD)	177,053.963	177,026.311	177,026.520	177,015.427	177,026.697	177,021.243
Best Cost (USD)	177,010.359	177,010.359	177,010.359	177,010.359	177,010.359	177,010.359
Worst Cost (USD)	177,286.754	177,064.779	177,064.779	177,061.038	177,064.903	177,064.779
Standard Deviation	81.170	24.386	24.689	15.204	24.957	21.768
Selection				O		
	60	**70**	**80**	**90**	**100**	**-**
Mean Cost (USD)	177,026.311	177,021.243	177,021.225	177,015.813	177,015.813	-
Best Cost (USD)	177,010.359	177,010.359	177,010.359	177,010.359	177,010.359	-
Worst Cost (USD)	177,064.779	177,064.779	177,068.339	177,064.903	177,064.903	-
Standard Deviation	24.386	21.768	21.793	16.363	16.363	-
Selection						-

Table 15. AF sensitivity analysis results and parameter value selection.

	0	15	30	45	60	75	90
Mean Cost (USD)	177,010.359	177,010.359	177,010.359	177,010.359	177,010.359	177,010.359	177,010.359
Best Cost (USD)	177,015.801	177,021.078	177,020.881	177,015.427	177,020.869	177,026.323	177,020.869
Worst Cost (USD)	177,064.779	177,064.779	177,064.903	177,061.038	177,064.779	177,064.903	177,064.779
Standard Deviation	16.326	21.440	21.062	15.204	21.036	24.406	21.036
Selection				O			
	105	**120**	**135**	**150**	**165**	**180**	**-**
Mean Cost (USD)	177,010.359	177,010.359	177,010.359	177,010.359	177,010.359	177,010.359	-
Best Cost (USD)	177,042.110	177,031.778	177,015.801	177,026.336	177,025.937	177,026.311	-
Worst Cost (USD)	177,064.903	177,064.903	177,064.779	177,064.903	177,064.779	177,064.779	-
Standard Deviation	25.958	26.253	16.326	24.425	23.815	24.386	-
Selection							-

5. Conclusions

In this study, an improved LCEA model was proposed to design an optimal WDS based on cost and energy, and performance was compared through the developed new resilience index. Using the specifications of the WDS under consideration and the regulations of the target watershed, a criterion was established to determine the Hazen–Williams coefficient, which serves as a basis for pipe renewal and replacement. The energy-based design has several advantages in that it aims to minimize energy consumption at all stages, including fabrication, maintenance, and disposal, due to the strength of the improved LCEA model. The energy-based design showed better performance than the cost-based design, especially in terms of energy recycling, which increased by approximately 36 times. Recycled energy, pointing to the energy benefits gained from the pipe rehabilitation and replacement process, had a positive impact on energy consumption. Additionally, the energy-based design demonstrated zero energy consumption for pipe repairs. As a result, the energy-based optimal design can consider a wide range of energy consumption aspects to achieve a more efficient design over the entire WDS life cycle.

To compare the performance of the proposed WDS design using the improved LCEA, an analysis was performed based on a new resilience index. As a result of analyzing the resilience index according to the scenario, it was confirmed that in most pipe failure scenarios, the energy-based optimal design showed better performance than the cost-based optimal design when pipe failure occurred. Based on the resilience index analysis results, it was found that the energy-based optimal design applied to a single-pipe failure scenario can respond to disaster more effectively than the cost-based optimal design when a pipe failure occurs.

The improved LCEA in this study relies on assumptions from prior research (e.g., energy consumption based on pipe diameter). To align better with real-world conditions, future studies should involve laboratory-scale experiments using the proposed equations. Further and extensive research can facilitate the practical application of the life cycle-based optimal design to actual drainage systems, allowing for the development of diverse optimal design techniques for various networks and objectives beyond energy.

Author Contributions: Y.m.R. and E.H.L. carried out the literature survey and drafted the manuscript. Y.m.R. worked on the subsequent draft of the manuscript. Y.m.R. performed the simulations. E.H.L. conceived the original idea of the proposed method. All authors have read and agreed to the published version of the manuscript.

Funding: This work was supported by Korea Environment Industry & Technology Institute (KEITI) through Technology development project to optimize planning, operation, and maintenance of urban flood control facilities Project, funded by Korea Ministry of Environment (MOE) (RS-2024-00398012).

Data Availability Statement: The data presented in this study are available on request from the corresponding author.

Conflicts of Interest: The authors declare no conflicts of interest.

References

1. Bolognesi, A.; Bragalli, C.; Marchi, A.; Artina, S. Genetic heritage evolution by stochastic transmission in the optimal design of water distribution networks. *Adv. Eng. Softw.* **2010**, *41*, 792–801. [CrossRef]
2. Diao, K.; Jung, D.; Farmani, R.; Fu, G.; Butler, D.; Lansey, K. Modular interdependency analysis for water distribution systems. *Water Res.* **2021**, *201*, 117320. [CrossRef] [PubMed]
3. Alperovits, E.; Shamir, U. Design of optimal water distribution systems. *Water Resour. Res.* **1977**, *13*, 885–900. [CrossRef]
4. Geem, Z.W. Optimal cost design of water distribution networks using harmony search. *Eng. Optim.* **2006**, *38*, 259–277. [CrossRef]
5. Shakhsi-Niaei, M.; Esfandarani, M.S. Multi-objective deterministic and robust models for selecting optimal pipe materials in water distribution system planning under cost, health, and environmental perspectives. *J. Clean. Prod.* **2019**, *207*, 951–960. [CrossRef]
6. Lansey, K.E.; Mays, L.W. Optimization model for water distribution system design. *J. Hydraul. Eng.* **1989**, *115*, 1401–1418. [CrossRef]
7. Reca, J.; Martínez, J. Genetic algorithms for the design of looped irrigation water distribution networks. *Water Resour. Res.* **2006**, *42*, W05416. [CrossRef]
8. Jung, D.; Kang, D.; Kim, J.H. Development of a hybrid harmony search for water distribution system design. *KSCE J. Civ. Eng.* **2018**, *22*, 1506–1514. [CrossRef]
9. Lee, E.H. Application of self-adaptive vision-correction algorithm for water-distribution problem. *KSCE J. Civ. Eng.* **2021**, *25*, 1106–1115. [CrossRef]
10. Ryu, Y.M.; Lee, E.H. Application of Modified Hybrid Vision Correction Algorithm for Water Distribution Systems in Civil Engineering. *KSCE J. Civ. Eng.* **2023**, *27*, 3617–3631. [CrossRef]
11. Lee, E.H.; Lee, H.M.; Yoo, D.G.; Kim, J.H. Application of a meta-heuristic optimization algorithm motivated by a vision correction procedure for civil engineering problems. *KSCE J. Civ. Eng.* **2018**, *22*, 2623–2636. [CrossRef]
12. Saldarriaga, J.; Páez, D.; Salcedo, C.; Cuero, P.; López, L.L.; León, N.; Celeita, D. A direct approach for the near-optimal design of water distribution networks based on power use. *Water* **2020**, *12*, 1037. [CrossRef]
13. Sangroula, U.; Han, K.H.; Koo, K.M.; Gnawali, K.; Yum, K.T. Optimization of water distribution networks using genetic algorithm based SOP–WDN program. *Water* **2022**, *14*, 851. [CrossRef]
14. Lee, S.; Yoo, D.G.; Jung, D.; Kim, J.H. Optimal life cycle design of water pipe system using genetic algorithm. *J. Korea Acad. -Ind. Coop. Soc.* **2015**, *16*, 4216–4227.
15. Risch, E.; Gutierrez, O.; Roux, P.; Boutin, C.; Corominas, L. Life cycle assessment of urban wastewater systems: Quantifying the relative contribution of sewer systems. *Water Res.* **2015**, *77*, 35–48. [CrossRef]
16. Shamir, U.; Howard, C.D. An analytic approach to scheduling pipe replacement. *J.-Am. Water Work. Assoc.* **1979**, *71*, 248–258. [CrossRef]
17. Sharp, W.W.; Walski, T.M. Predicting internal roughness in water mains. *J.-Am. Water Work. Assoc.* **1988**, *80*, 34–40. [CrossRef]
18. Mononobe, N. Hydraulics. *Iwanami* **1960**, 155–158.
19. Male, J.W.; Walski, T.M.; Slutsky, A.H. Analyzing water main replacement policies. *J. Water Resour. Plan. Manag.* **1990**, *116*, 362–374. [CrossRef]
20. Kleiner, Y.; Adams, B.J.; Rogers, J.S. Long-term planning methodology for water distribution system rehabilitation. *Water Resour. Res.* **1988**, *34*, 2039–2051. [CrossRef]
21. Filion, Y.R.; MacLean, H.L.; Karney, B.W. Life-cycle energy analysis of a water distribution system. *J. Infrastruct. Syst.* **2004**, *10*, 120–130. [CrossRef]
22. Todini, E. Looped water distribution networks design using a resilience index based heuristic approach. *Urban Water* **2000**, *2*, 115–122. [CrossRef]

23. Cimellaro, G.P.; Tinebra, A.; Renschler, C.; Fragiadakis, M. New resilience index for urban water distribution networks. *J. Struct. Eng.* **2016**, *142*, C4015014. [CrossRef]
24. Choi, Y.H.; Lee, H.M.; Yoo, D.G.; Kim, J.H. Optimal design of water supply system using multi-objective harmony search algorithm. *J. Korean Soc. Water Wastewater* **2015**, *29*, 293–303. [CrossRef]
25. Mandl, C.E. A survey of mathematical optimization models and algorithms for designing and extending irrigation and wastewater networks. *Water Resour. Res.* **1981**, *17*, 769–775. [CrossRef]
26. Monbaliu, J.; Jo, J.; Fraisse, C.W.; Vadas, R.G. Computer aided design of pipe networks. *Tech. Rev. -Mitsubishi Heavy Ind.* **1990**, *2*, 789–797.
27. Gessler, J.; Walski, T.M. *Water Distribution System Optimization (No. WES/TR/EL-85-11)*; Army Engineer Waterways Experiment Station Vicksburg MS Environmental Lab: Vicksburg, MA, USA, 1985.
28. Su, Y.C.; Mays, L.W.; Duan, N.; Lansey, K.E. Reliability-based optimization model for water distribution systems. *J. Hydraul. Eng.* **1987**, *113*, 1539–1556. [CrossRef]
29. Vasan, A.; Simonovic, S.P. Optimization of water distribution network design using differential evolution. *J. Water Resour. Plan. Manag.* **2010**, *136*, 279–287. [CrossRef]
30. Geem, Z.W.; Kim, J.H.; Loganathan, G.V. A new heuristic optimization algorithm: Harmony search. *Simulation* **2001**, *76*, 60–68. [CrossRef]
31. Maier, H.R.; Simpson, A.R.; Zecchin, A.C.; Foong, W.K.; Phang, K.Y.; Seah, H.Y.; Tan, C.L. Ant colony optimization for design of water distribution systems. *J. Water Resour. Plan. Manag.* **2003**, *129*, 200–209. [CrossRef]
32. Reca, J.; Martínez, J.; Gil, C.; Baños, R. Application of several meta-heuristic techniques to the optimization of real looped water distribution networks. *Water Resour. Manag.* **2008**, *22*, 1367–1379. [CrossRef]
33. Baek, C.W. Development of Optimal Decision-Making System for Rehabilitation of Water Distribution Systems Using ReHS. Master's Thesis, Korea University, Seoul, Republic of Korea, 2002.
34. Kim, J.H.; Kim, T.G.; Kim, J.H.; Yoon, Y.N. A study on the pipe network system design using non-linear programming. *J. Korean Water Resour. Assoc.* **1994**, *27*, 59–67.
35. Menon, K.K.; Narulkar, S.M. Application of heuristic-based algorithm in water distribution network design. *J. Water Resour. Pollut. Stud.* **2016**, *1*, 1–14.
36. U.S. Environmental Protection Agency (US EPA). *EPANET 2.0 User's Manual*; US EPA: Washington, DC, USA, 2000.
37. Jinesh Babu, K.S.; Mohan, S. Extended period simulation for pressure-deficient water distribution network. *J. Comput. Civ. Eng.* **2012**, *26*, 498–505. [CrossRef]
38. Mahmoud, H.A.; Savić, D.; Kapelan, Z. New pressure-driven approach for modeling water distribution networks. *J. Water Resour. Plan. Manag.* **2017**, *143*, 04017031. [CrossRef]
39. Hamed, M.M.; Elsayad, M.A.; Mahfouz, S.Y.; Khadr, W.M.H. Graphical user interface for water distribution network pressure-driven analysis using artificial elements. *Sustain. Water Resour. Manag.* **2022**, *8*, 89. [CrossRef]
40. Khadr, W.M.H.; Hamed, M.M.; Nashwan, M.S. Pressure Driven analysis of water distribution systems for preventing siphonic flow. *J. Hydro-Environ. Res.* **2022**, *44*, 102–109. [CrossRef]
41. Lee, S.Y. Research on Life Cycle Energy Analysis of Water Distribution System. Master's Thesis, Korea University, Seoul, Republic of Korea, 2014.
42. Korea Energy Economics Institute. Available online: https://www.keei.re.kr/main.nsf/index.html?open&p=/web_keei/change.nsf/UnitConverF&s=?OpenForm (accessed on 25 August 2023).
43. Korean Statistical Information Service. Available online: https://kosis.kr/statHtml-/statHtml.do?orgId=388&tblId=TX_38804_A010 (accessed on 25 August 2023).
44. Beker, B.A.; Kansal, M.L. Fuzzy logic-based integrated performance evaluation of a water distribution network. *AQUA—Water Infrastruct. Ecosyst. Soc.* **2022**, *71*, 490–506. [CrossRef]
45. Jung, D.; Kang, D.; Kim, J.H.; Lansey, K. Robustness-based design of water distribution systems. *J. Water Resour. Plan. Manag.* **2014**, *140*, 04014033. [CrossRef]
46. Pagano, A.; Sweetapple, C.; Farmani, R.; Giordano, R.; Butler, D. Water distribution networks resilience analysis: A comparison between graph theory-based approaches and global resilience analysis. *Water Resour. Manag.* **2019**, *33*, 2925–2940. [CrossRef]
47. Rossman, L.; Woo, H.; Tryby, M.; Shang, F.; Janke, R.; Haxton, T. *EPANET 2.2 User Manual*; Report EPA/600/r-20/133; Environmental Protection Agency: Washington, DC, USA, 2020.
48. Yoon, J.S.; Yoo, D.G.; Lee, H.M.; Kim, J.H. Optimal leakage detection model of water distribution systems using semi-pressure driven analysis and harmony search. *J. Korean Soc. Hazard Mitig.* **2012**, *12*, 23–32. [CrossRef]